Sheridan et al. Supplemental Figures

A

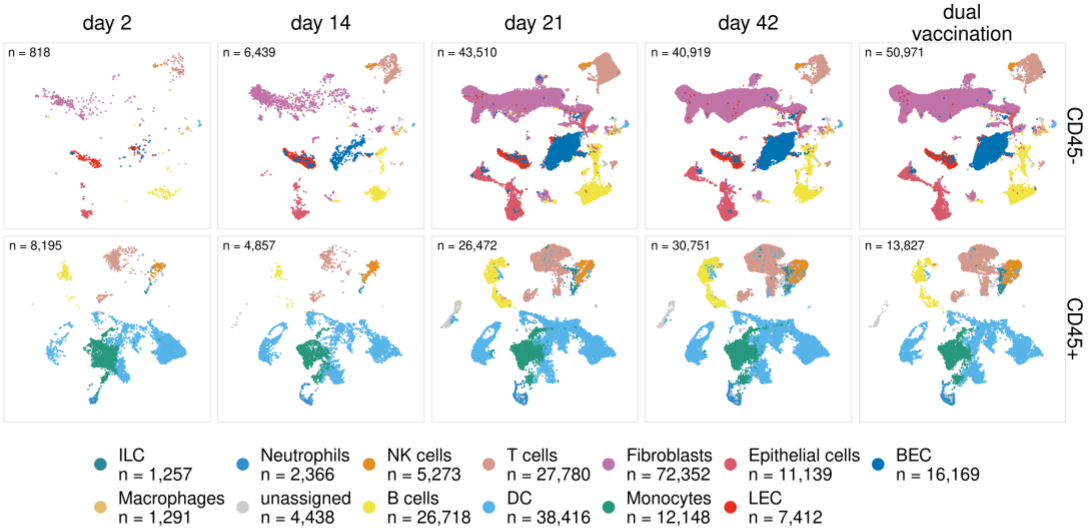

B

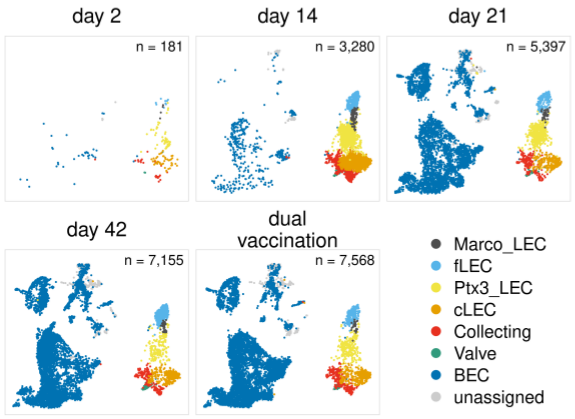

C

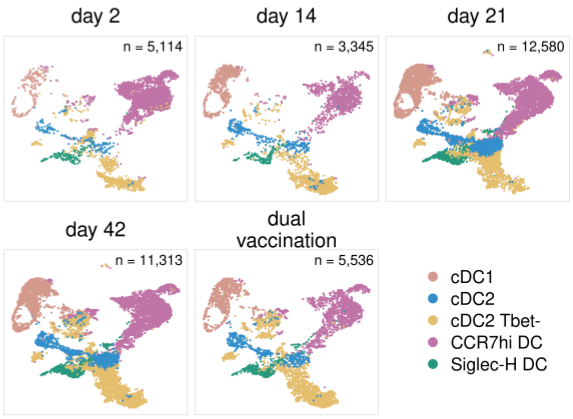

D

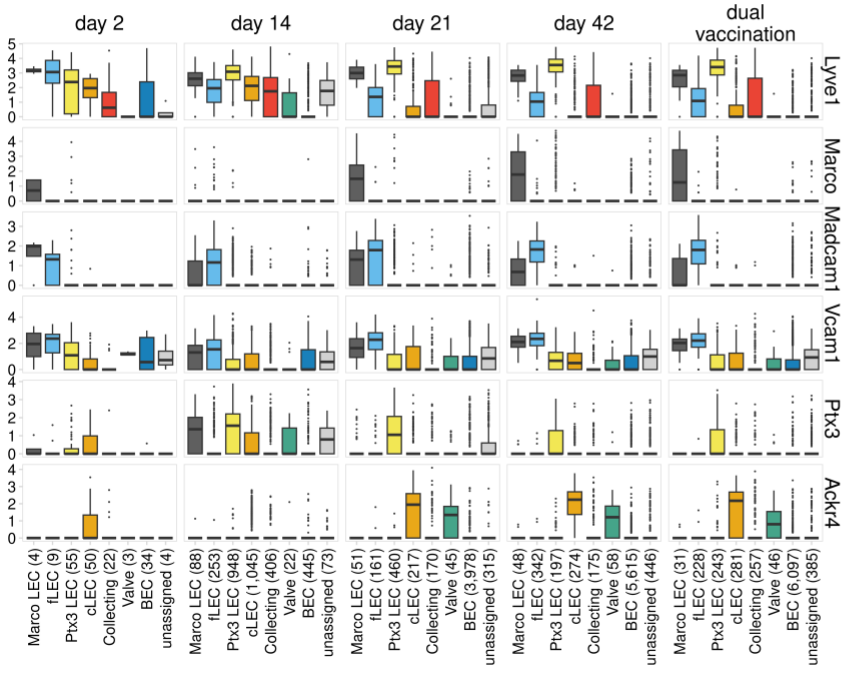

E

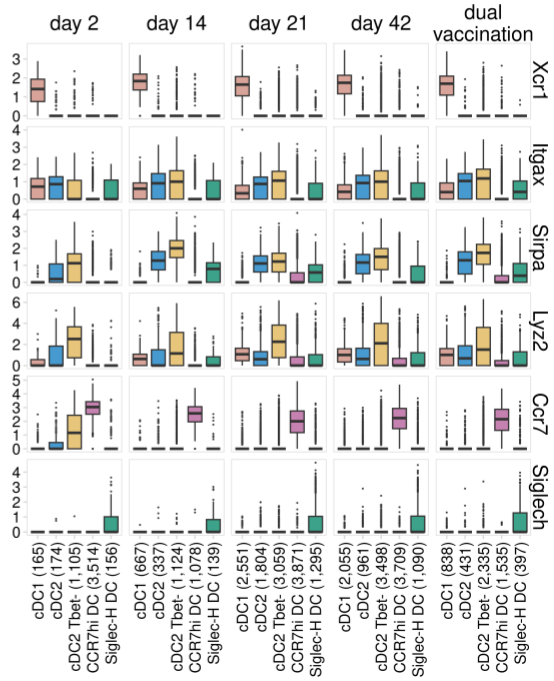

Sheridan et al. Supplemental Figures

Supplemental Figure 1.

A. UMAP projections show cell types identified for CD45- and CD45+ samples.
B. UMAP projections show LEC subsets identified for each timepoint.
C. UMAP projections show DC subsets identified for each timepoint.
D. The expression of key marker genes is shown for LEC subsets.
E. The expression of key marker genes is shown for DC subsets.

Sheridan et al. Supplemental Figures

A

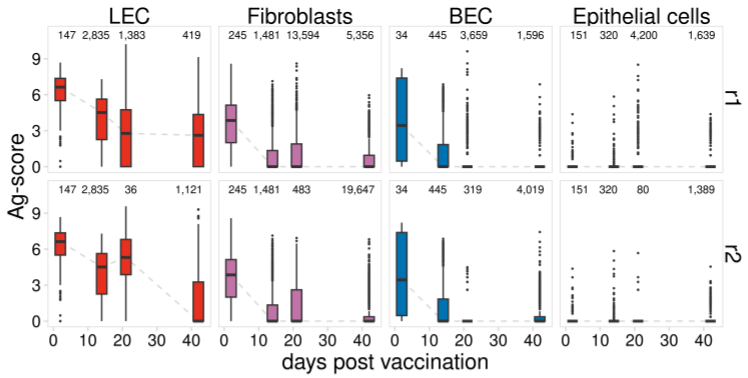

B

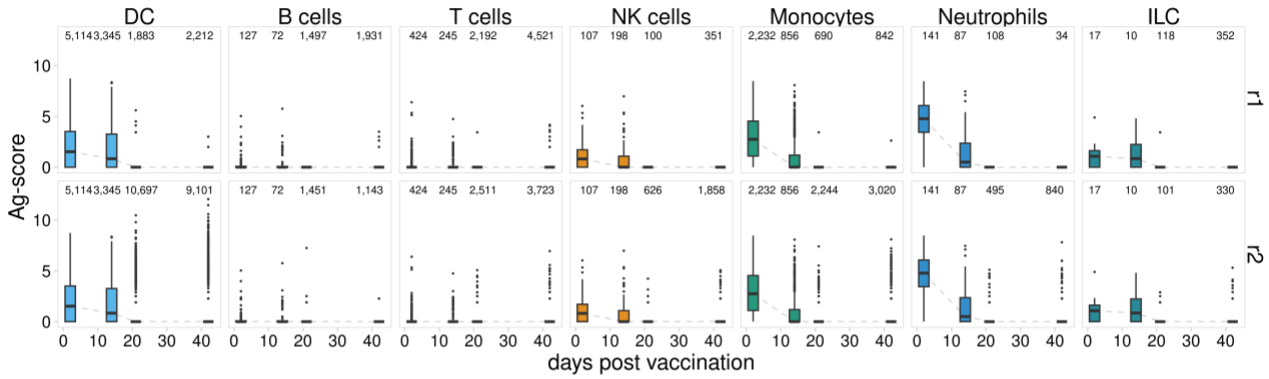

C

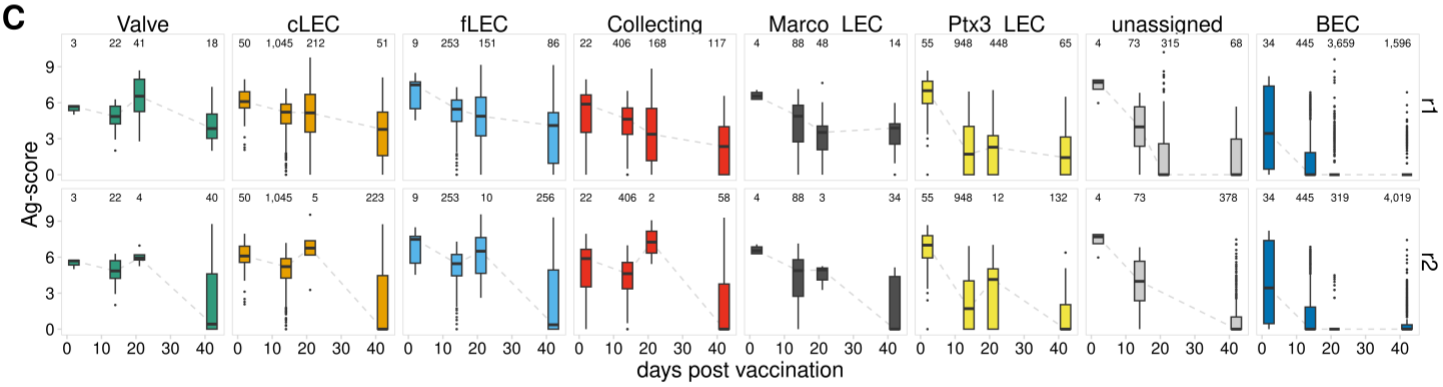

D

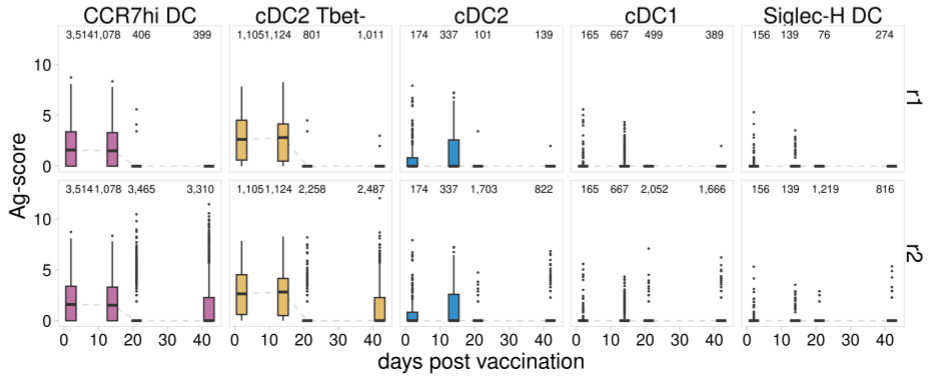

Supplemental Figure 2.

A. Ag-scores are shown for each timepoint for CD45- cell types. Two biological replicates are shown for the day 21 and day 42 timepoints (r1, r2), one biological replicate is shown for the day 2 and day 14 timepoints (this replicate is plotted for both r1 and r2). The number of cells identified for each cell type is shown above each timepoint.
B. Ag-scores are shown for each timepoint for CD45+ cell types, as described in A.
C. Ag-scores are shown for each timepoint for LEC subsets, as described in A.
D. Ag-scores are shown for each timepoint for DC subsets, as described in A.

Sheridan et al. Supplemental Figures

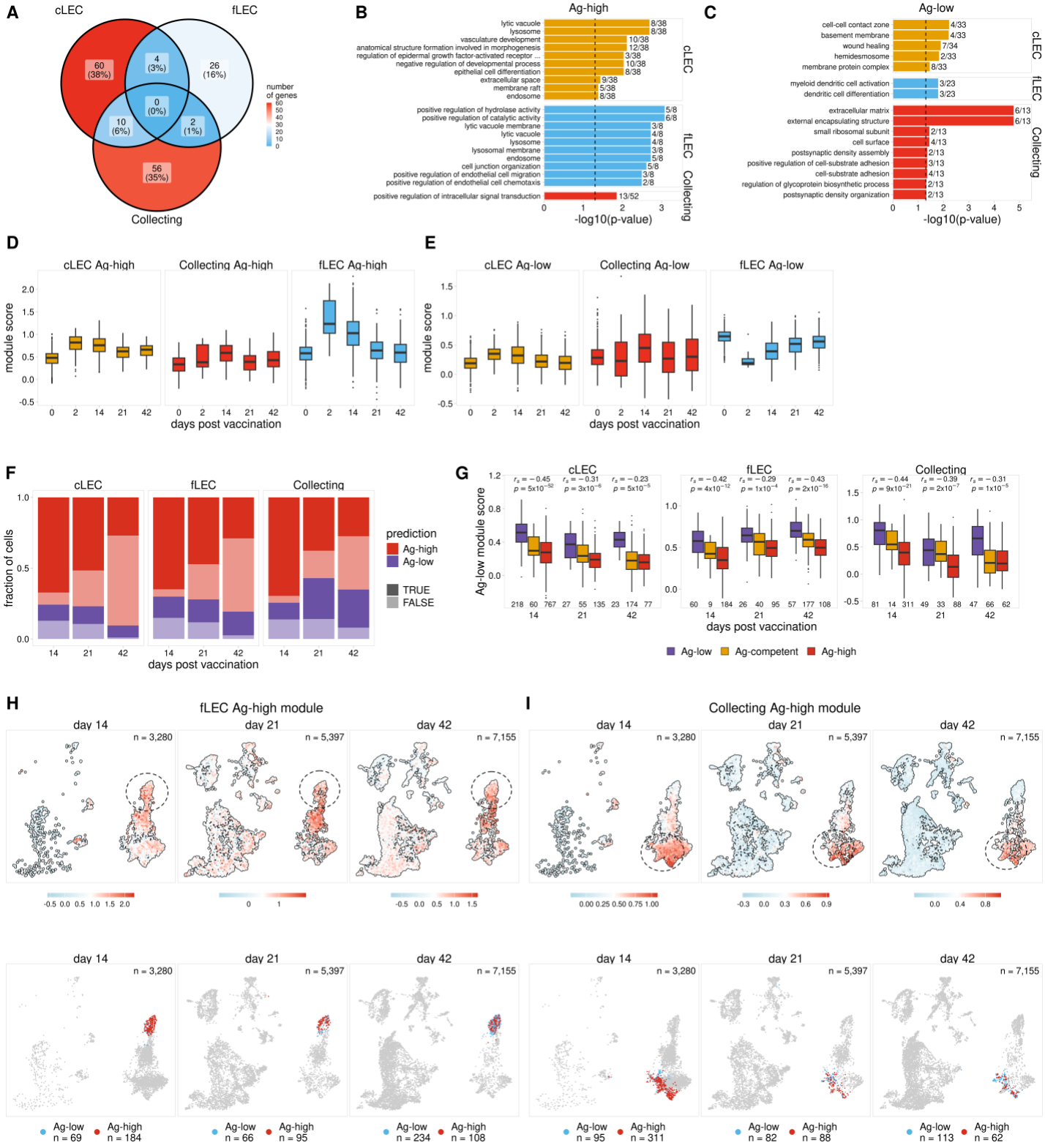

Supplemental Figure 3.

A. Venn diagram shows the number of genes shared between the cLEC, fLEC and collecting LEC gene modules.
B. The top gene ontology terms (biological process, cellular component) are shown for the cLEC, fLEC, and collecting LEC Ag-high gene modules. The number of overlapping genes is shown to the right of each ontology term.
C. Top gene ontology terms are shown for Ag-low gene modules as described in A.
D. The expression of each Ag-high gene module is shown for naive LECs (0 days post vaccination) along with each time point.
E. The expression of each Ag-low gene module is shown as described in C.
F. The fraction of cells predicted to be Ag-low and Ag-high is shown for each LEC subset.
G. Ag-low module score is shown for Ag-low, Ag-high, and predicted Ag-competent LECs. The Spearman correlation between Ag classes and Ag-high module score is shown for each timepoint. One-sided p values were calculated and adjusted using Benjamini-Hochberg correction. The number of cells plotted is shown below each boxplot.
H. UMAP projections show fLEC Ag-high module scores for each timepoint.
I. UMAP projections show collecting LEC Ag-high module scores for each timepoint.

Sheridan et al. Supplemental Figures

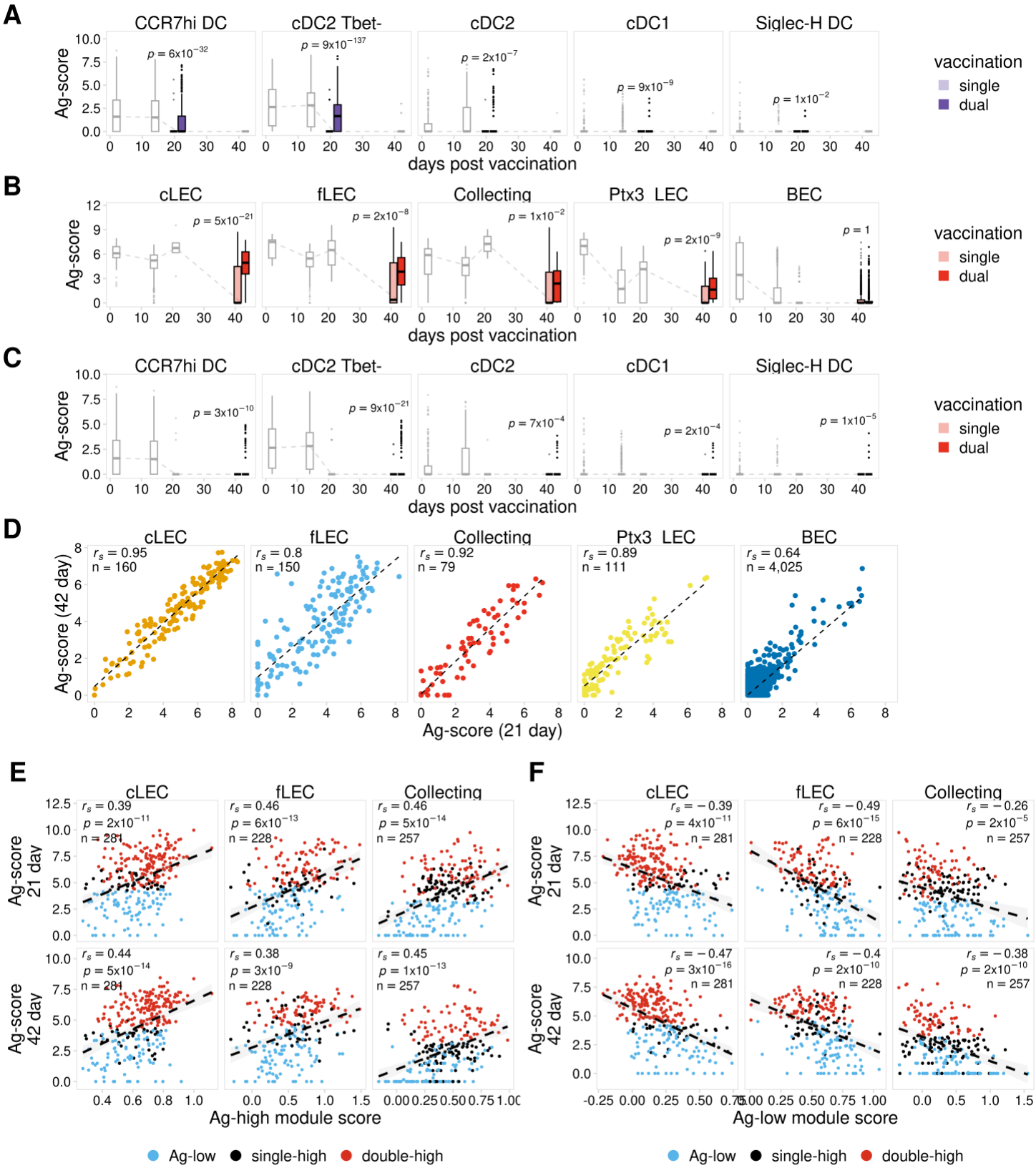

Supplemental Figure 4

A. Ag-score is shown for single and dual vaccinations for the 21 day timepoint for DC subsets from a biological replicate. This analysis was not performed for a biological replicate for LEC subsets due to the low number of LECs recovered (<40 total cells). Other timepoints are shown in grey. P values were calculated using a one-sided Wilcoxon rank sum test with Benjamini-Hochberg correction.
B. Ag-score is shown for the 42 day timepoint for LEC subsets from a biological replicate, as described in A.
C. Ag-score is shown for the 42 day timepoint for DC subsets from a biological replicate, as described in A.
A. 21 day and 42 day Ag-score is compared for LEC subsets from a biological replicate.

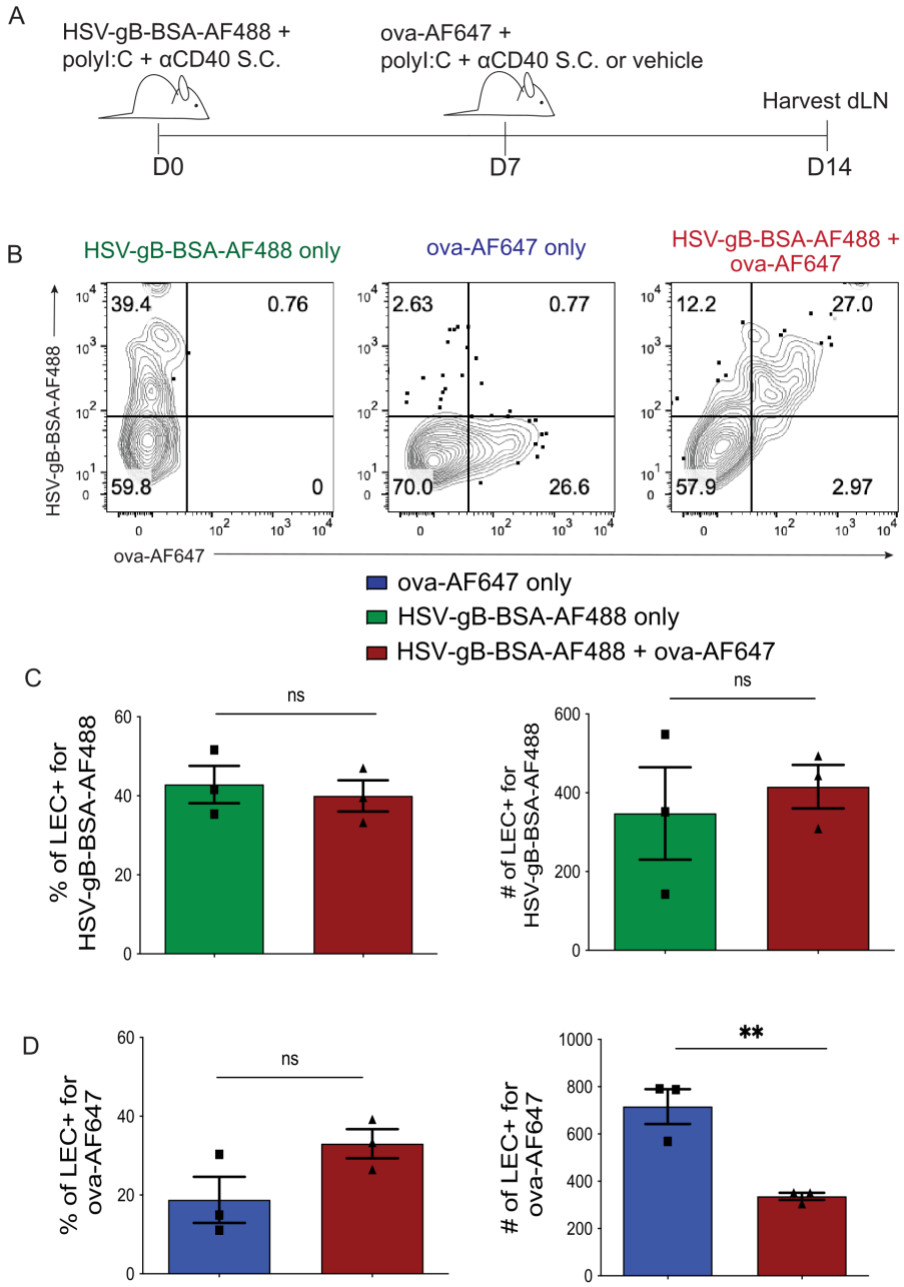

Supplemental Figure 5.

A. Mice were immunized subcutaneously with 10 μg of HSV-gB-BSA-AF488, 5 μg of polyI:C, and 5 μg αCD40 in the footpads. After 7 days, mice were immunized with 10 mg of ova-AF647, 5 mg of polyI:C, and aCD40 in the same location. Mice were sacrificed a week later and draining popliteal LN were harvested.
B. Representative flow plots of respective treatments after gating on LEC (CD45-PDPN+CD31+).
C. Quantification of the percent and total number of LEC that are positive for HSV-gB-BSA-AF88 in mice immunized with only HSV-gB-BSA-AF488 (green bar) or mice immunized with HSV-gB-BSA-AF488 and ova-AF647 (red bar).
D. Quantification of the percent and total number of LEC that are positive for ova-AF647 in mice immunized with only ova-AF647 (blue bar) or HSV-gB-BSA-AF488 and ova-AF647 (red bar). Statistical analysis was done using an unpaired t-test where the p-value of the single-immunized mice and dual-immunized mice was <0.0001. Errors bars are mean ± standard error of the mean. In each experiment, at least n=3 mice per group were evaluated and the experiment was repeated n=5 times with similar results. Shown is the data from one of the experiments.

Sheridan et al. Supplemental Figures

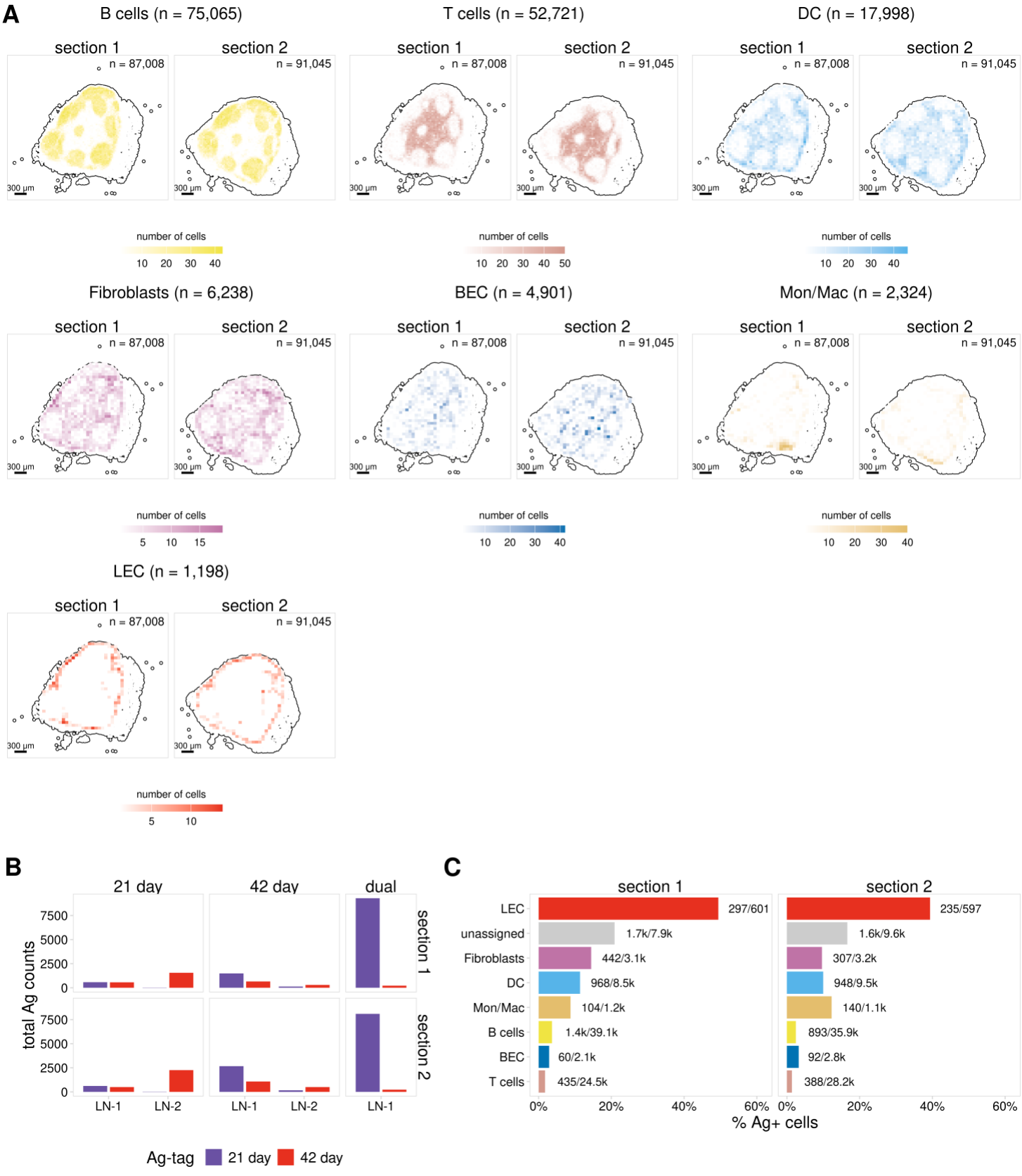

Supplemental Figure 6

A. Localization of annotated cell types is shown for replicate tissue sections analyzed with the Xenium platform. Annotated cell types with >100 identified cells are shown. Color indicates cell density.
B. Total Ag counts are shown for the 21 day and 42 day Ag tags, for mice immunized with the 21 day tag (left), 42 day tag (middle), or both 21 and 42 day tags (right). For each immunization group, tissue sections were analyzed for two LNs from separate mice (LN-1, LN-2), with the exception of the dual-immunization group. For each LN, two adjacent tissue sections were analyzed (section 1, section 2).
C. The fraction of Ag+ cells is shown for each cell type for tissue sections shown in Figure 4A.

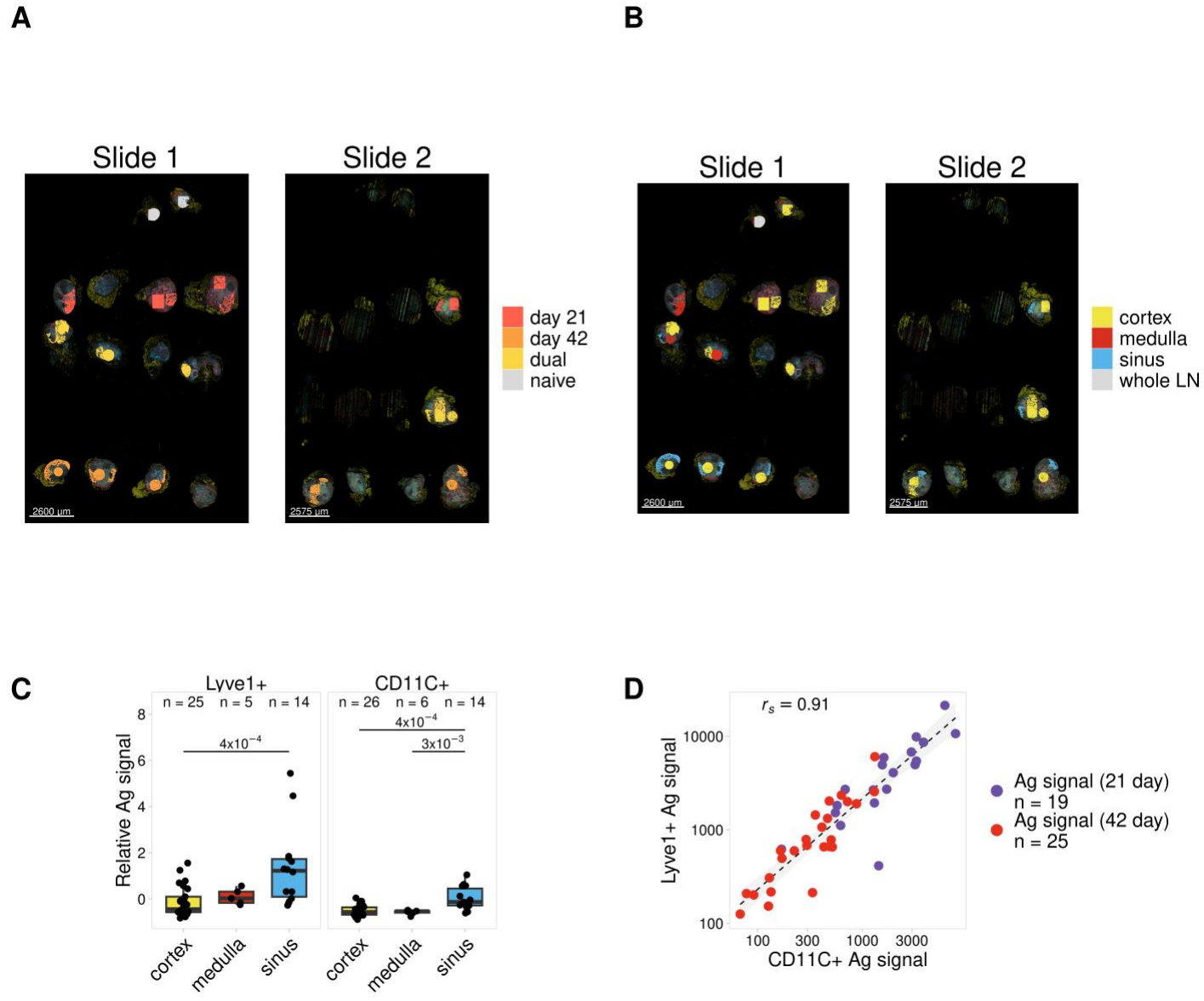

Supplemental Figure 7

A. Sample identity is shown for all regions analyzed using the GeoMx DSP platform.
B. Annotated regions are shown as described in A.
C. Relative antigen tag signal is shown for each sample and each region segmented based on Lyve1 (LECs) and CD11C (DCs). Normalized 21 day antigen signal was scaled across all regions from 21 day mice and dual immunized mice, 42 day antigen signal was scaled across all regions from 42 day mice and dual immunized mice. The number of plotted segments is shown above each boxplot. P values were calculated using a one-sided Wilcoxon rank sum test with Benjamini-Hochberg correction, p values <0.05 are shown.
D. Normalized antigen tag signal is shown for regions that included both Lyve1+ and CD11C+ segments. 21 day antigen signal is shown for 21 day and dual immunized mice, 42 day signal is shown for 42 day and dual immunized mice. The Spearman correlation coefficient is shown.

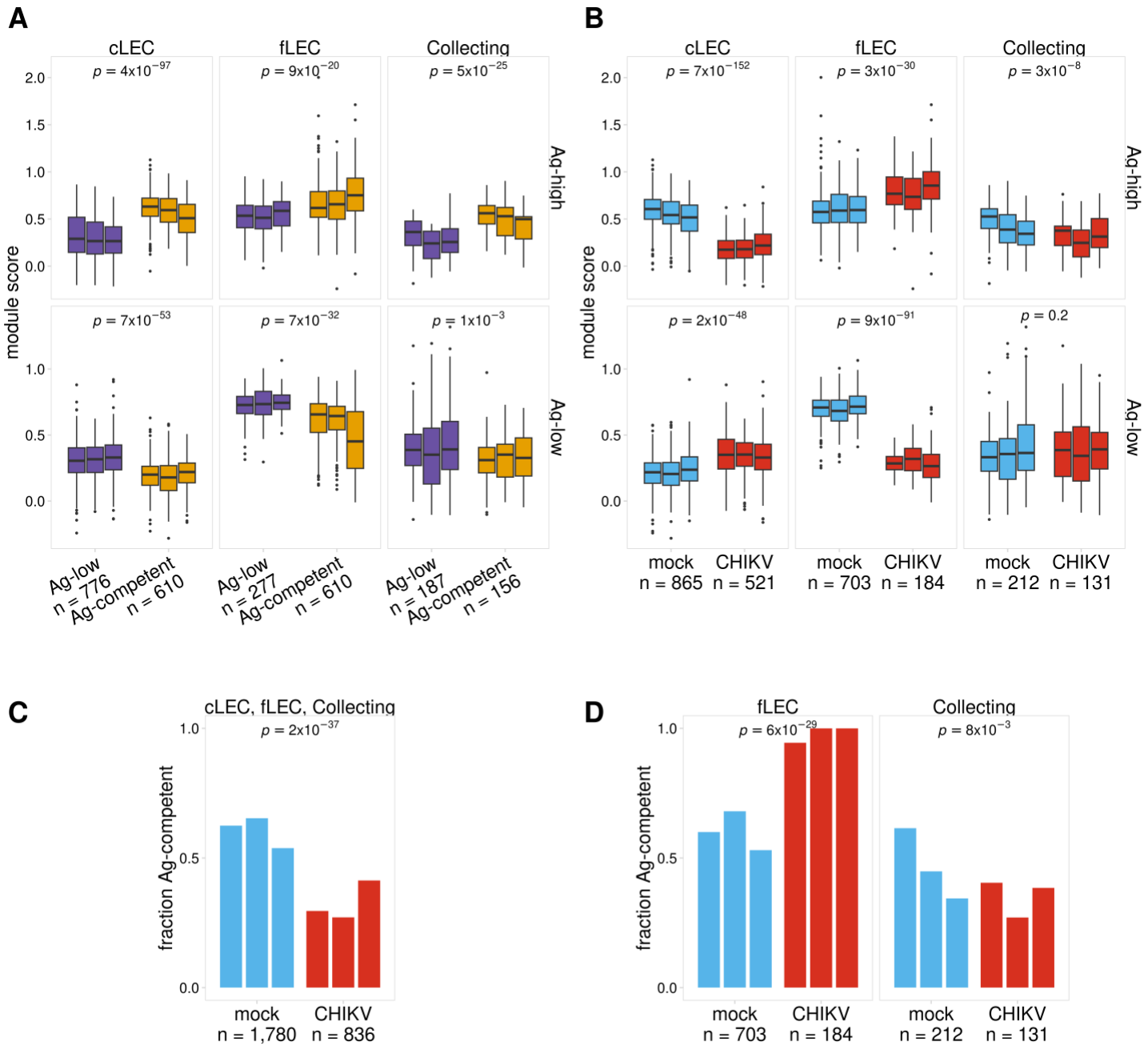

Supplemental Figure 8

A. Ag-high and Ag-low module scores are shown for the predicted Ag classes. P values were calculated using a two-sided Wilcoxon rank sum test with Benjamini-Hochberg correction.
B. Ag-high and Ag-low module scores are shown for mock and CHIKV-infected mice for each biological replicate. P values were calculated using a two-sided Wilcoxon rank sum test with Benjamini-Hochberg correction.
C. The total fraction of cLECs, fLECs, and collecting LECs predicted to be Ag-competent is shown for mock and CHIKV-infected mice for each biological replicate. P values were calculated using Fisher's exact test with Benjamini-Hochberg correction.
D. The fraction of fLECs and collecting LECs predicted to be Ag-competent is shown as described in C.

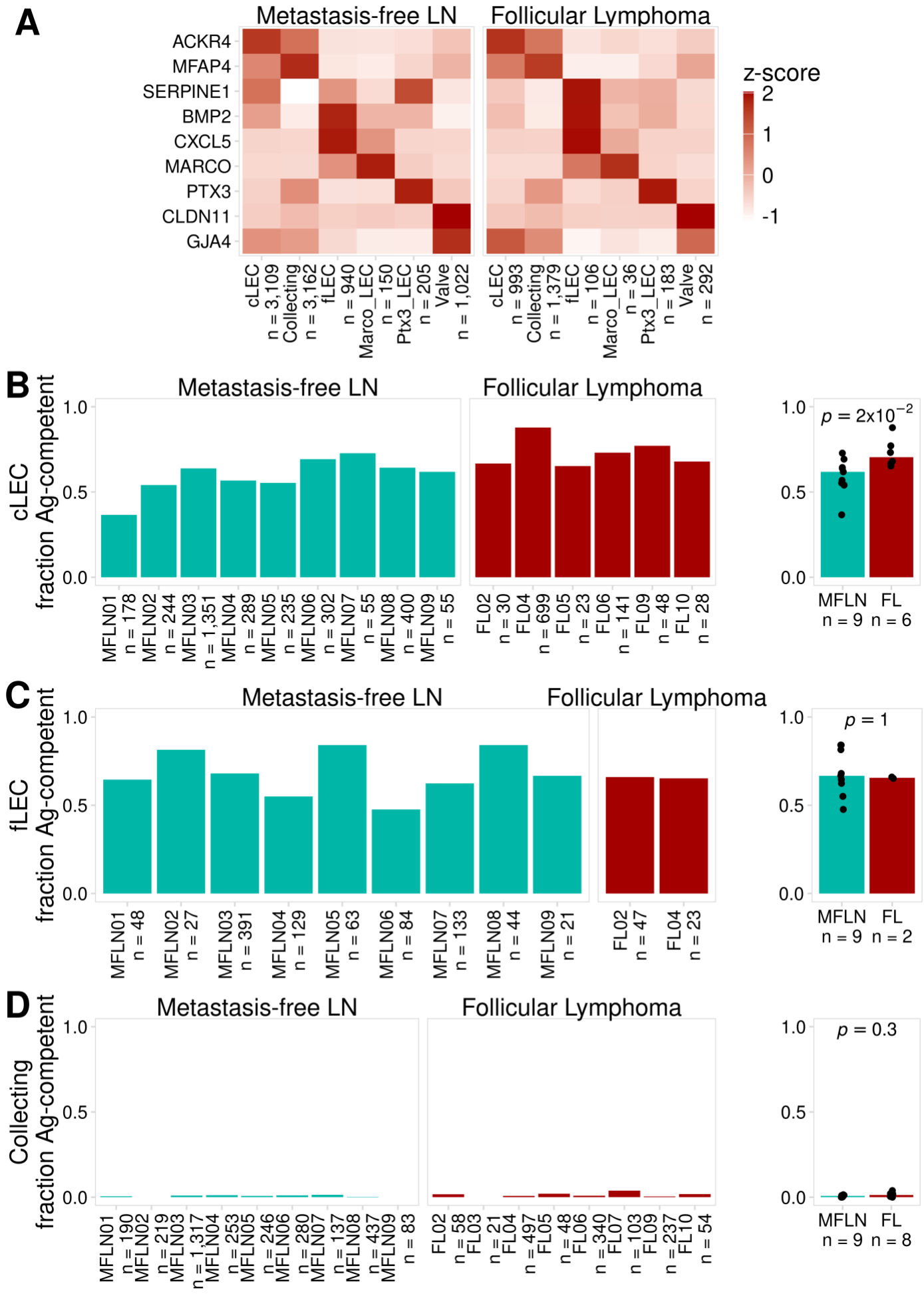
A
Metastasis-free LN
Follicular Lymphoma
ACKR4
MFAP4
SERPINE1
BMP2
CXCL5
MARCO
PTX3
CLDN11
GJA4
z-score
2
1
0
-1
cLEC n = 3,109
Collecting n = 3,162
fLEC n = 940
Marco_LEC n = 150
Ptx3_LEC n = 205
Valve n = 1,022
cLEC n = 993
Collecting n = 1,379
fLEC n = 106
Marco_LEC n = 36
Ptx3_LEC n = 183
Valve n = 292
B
cLEC fraction Ag-competent
Metastasis-free LN
Follicular Lymphoma
1.0
0.5
0.0
MFLN01 n = 178
MFLN02 n = 244
MFLN03 n = 1,351
MFLN04 n = 289
MFLN05 n = 235
MFLN06 n = 302
MFLN07 n = 55
MFLN08 n = 400
MFLN09 n = 55
FL02 n = 30
FL04 n = 699
FL05 n = 23
FL06 n = 141
FL09 n = 48
FL10 n = 28
p = 2x10−2
MFLN n = 9
FL n = 6
C
fLEC fraction Ag-competent
Metastasis-free LN
Follicular Lymphoma
MFLN01 n = 48
MFLN02 n = 27
MFLN03 n = 391
MFLN04 n = 129
MFLN05 n = 63
MFLN06 n = 84
MFLN07 n = 133
MFLN08 n = 44
MFLN09 n = 21
FL02 n = 47
FL04 n = 23
p = 1
MFLN n = 9
FL n = 2
D
Collecting fraction Ag-competent
Metastasis-free LN
Follicular Lymphoma
MFLN01 n = 190
MFLN02 n = 219
MFLN03 n = 1,317
MFLN04 n = 253
MFLN05 n = 246
MFLN06 n = 280
MFLN07 n = 137
MFLN08 n = 437
MFLN09 n = 83
FL02 n = 58
FL03 n = 21
FL04 n = 497
FL05 n = 48
FL06 n = 340
FL07 n = 103
FL09 n = 237
FL10 n = 54
p = 0.3
MFLN n = 9
FL n = 8

Supplemental Figure 9

A. Mean expression is shown for LEC marker genes for metastasis-free control lymph node (MFLN) and follicular lymphoma (FL) samples from Abe et al.
B. The fraction of cLECs predicted to be Ag-competent is shown for each MFLN and FL sample with at least 20 identified cLECs (left). P values were calculated using a two-sided Wilcoxon rank sum test with Benjamini-Hochberg correction (right).
C. The fraction of fLECs predicted to be Ag-competent is shown as in A.
D. The fraction of collecting LECs predicated to be Ag-compentent is shown as in A.